International Specialty Conference on Cold-Formed Steel Structures

(2010) - 20th International Specialty Conference on Cold-Formed Steel Structures

Nov 3rd, 12:00 AM

Strength Prediction Model for Power Acutated Fasteners Connecting Steel Members in Tension and Shear-north American Applications

J. R. Ubejd Mujagic

Perry S. Green

William G. Gould

Twentieth International Specialty Conference on Cold-Formed Steel Structures
St. Louis, Missouri, U.S.A., November 3 & 4, 2010

Strength Prediction Model for Power Actuated Fasteners Connecting Steel Members in Tension and Shear– North American Applications

J.R. Ubejd Mujagic,[1] Perry S. Green[2] and William G. Gould[3]

ABSTRACT

Power-actuated fasteners (PAFs), also referred to as pins, are small nail-like or threaded stud type connectors. They can be used in conjunction with several materials and in a number of different applications. Typical applications in steel include attachments of deck sheeting or diaphragms, architectural or mechanical components, or miscellaneous support brackets or connections to supporting steel members. Traditionally, the design strength of the connections featuring power-actuated fasteners has been determined through standardized testing protocols. In the United States, this protocol is embodied in the American Society for Testing and Materials (ASTM) Standard E 1190. The purpose of this study was to create a generic strength prediction model for pins embedded in steel substrate and subjected to either shear or tension, and to present the equations in a limit states format applicable to the North American practice and applications.

1 INTRODUCTION

The purpose of this study was to create a generic and comprehensive strength prediction model for power-actuated fasteners (PAFs) embedded in steel substrate and subjected to either shear or tension. Although strength

[1]Structural Engineering Consultant, Atlanta, GA
[2]Consultant, Former Technical Director, SJI, Myrtle Beach, SC
[3]Director of Engineering, HILTI, Tulsa, OK

provisions for PAFs exist in European practice, as embodied by EN 1993-1-3 (ECS 2006), they were not able to be directly incorporated into North American practice given differences in definitions of nominal strength, safety and reliability related adjustments, and somewhat different scope compared to the data available as a part of this study. However, EN 1993-1-3 Table 8.3 provided valuable guidance to this study with respect to the definition of limit states, scope, etc. Therefore, a separate effort, as described in the following sections was required to provide an acceptable and generic strength prediction model for PAFs.

Typical applications in steel include attachments of deck sheathing or diaphragms, architectural or mechanical components, or miscellaneous support brackets or connections to the supporting steel members. Typical fasteners used in conjunction with steel embedment are shown in Figure 1 (HILTI 2009).

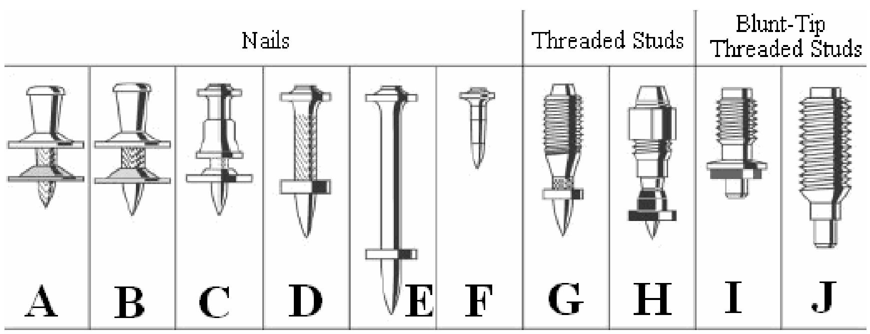

Figure 1 Typical Pin Types (HILTI 2009)

PAFs plastically deform and displace the embedment material when installed into it. Connection strength in tension is derived from the propensity of the displaced material to partially return to its original position. Specifically, this tendency on the part of the displaced material creates hoop stresses around the perimeter of the embedded fastener which results in friction forces resisting pullout. In addition to this tension strength mechanism, high temperatures developed during fastener driving into an embedment substrate cause the surface of the fastener to be partially fused with the surrounding substrate (Beck et al. 2003), providing additional resistance against pull-out. Alternatively, a PAF connection loaded in tension could also fail by fastener fracture and sheet pull-over over the fastener head. One of the most instrumental properties for the

PAF penetration into embedment steel is its hardness. To successfully penetrate the substrate material, fasteners must have a hardness of 4 to 5 times the embedment material (Beck & Reuter 2005), and are usually manufactured with Rockwell C scale (HRC) hardness between 49 and 58, depending on intended application and fastener geometry. Hardness increases with increasing content of carbon in steel. Typical pre-hardened steels used in manufacturing of PAFs are AISI 1060, 1070 and 1080, as defined in ASTM A 29 (ASTM 2008a), although different proprietary steel types may exist. In shear, the PAF connection could fail by shear fracture of the fastener, bearing failure of the connected substrate, tilting of the fastener followed by its pullout in shear, or by fracture of the connected net section including block shear.

Traditionally, the design strength of connections featuring PAFs has been determined through standardized testing protocols. In the United States, this protocol is embodied in the American Society for Testing and Materials (ASTM) Standard E 1190. Acceptability of the strengths established by following this standardized testing protocol, must then be established for construction through an evaluation process under the auspices of International Code Council Evaluation Services (ICC-ES). The acceptance criteria (AC) for PAFs are established in ICC-ES document AC70 (2010). Among other aspects, AC70 stipulates acceptable testing procedures (i.e., ASTM E 1190), establishment of proper material limitations, application limitations, establishment of combined loading limit states, and determination of factors of safety. A separate evaluation is required for each PAF type, each application, each connection configuration, as well as the geometry of each fastener. Strength values determined for any given PAF satisfying the corresponding AC and reduced by an appropriate factor of safety are then provided in published manufacturer's catalogs, and are then available to be used in design.

2 OBJECTIVE, APPROACH AND SCOPE

As noted above, the objective of the study was to generate a strength prediction model, whereby the design strength of connections featuring PAFs embedded in steel substrates, loaded in shear and tension, can be numerically determined for any applicable limit state.

Test reports containing test data for PAFs embedded in a steel substrate and loaded in shear and tension were provided by four of the major product manufacturers of fasteners in North America: HILTI (2009, 2010), ITW Ramset (2009), Power Fasteners (2009) and Simpson Fasteners (2009). All the test reports submitted by the manufacturers document the tests performed in accordance with ASTM E 1190, thus eliminating variation in test data among different reports caused by any slight differences in their respective test setups.

The approach taken was to isolate tests featuring a specific loading condition (shear or tension) mode of failures in separate groups of data, and then generate a strength prediction model for each of the applicable failure modes. The design strength was then established based on the governing mode of failure for any given connection configuration, similar to the strength determination model for screws presently contained in the North American Specification for the Design of Cold-Formed Steel Structural Members, S100 (AISI 2007). The test data with incomplete, conflicting, or obviously flawed information was excluded.

3 TENSION LIMIT STATES

The modes of failure observed in tensile PAF tension test reports are PAF pull-out, tensile fracture, and sheet pull-over. The subsequent sections discuss each of the applicable limit states, and the analysis pertaining thereto. Various geometric variables used in this and other sections of this text are illustrated in Figure 2.

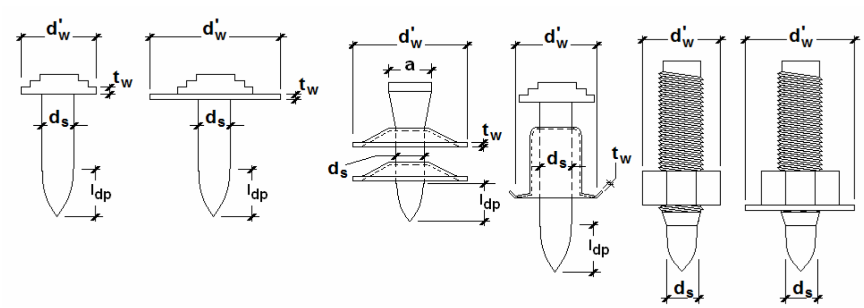

Figure 2 PAF Geometric Variables Used in the Strength Prediction Model

3.1 PAF FRACTURE IN TENSION

Tension fracture failures in PAFs embedded in steel are relatively rare. In fact, out of 1623 tension tests available to this study, only 10 specimens, with diameters of 0.146 and 0.150 in., experienced this mode of failure. This failure mode, however, is viable, and must be considered in practical design. Computing tensile strength, P_{tp}, is a trivial matter from a theoretical standpoint, and can be readily accomplished with Eq. 1.

$$P_{tp} = (d_s / 2)^2 \pi F_{uh} \qquad \text{(Eq. 1)}$$

Where:

d_s = diameter of PAF shank, in.
F_{uh} = ultimate tensile strength of hardened PAF steel, psi

The nominal values of F_{uh} can be found only in some manufacturer's catalogs (ITW Ramset 2007) and are commonly not indicated in the test reports. However, HRC values are generally reported in most manufacturers' catalogs and all test reports, including those available to this study. There are several published works and standards relating various hardness scales to ultimate tensile strength, including ASTM A 370 (ASTM 2009). A formula relating the two generally takes the shape of Eq. 2, where ρ and ζ are constants derived through regression of available data. It was found that for the data available to this study, the best fit is provided by ρ = 66000 and ζ = 1/40, which closely relates to the data published in BS 860:1967 (BSI 1967). Given the limited data sample of tension fracture tests, this validation was performed on shear fracture tests (Sec. 4.1), by relating shear and tension fracture strength by a factor of 0.6.

$$F_{uh} = \rho e^{(HRC / \zeta)} \qquad \text{(Eq. 2)}$$

It should be noted that a range of tensile strengths derived by this expression based on typical range of HRC values found in PAFs is very small. Therefore, and also considering inherent statistical scatter, very little can be gained in view of accuracy by using Eq. 2 over simply using a uniform average value of F_{uh} of 260 ksi over the range of HRC values from 52 to 56, which is the array of values seen in this study. Considering the limited database of 10 tests performed on two different fasteners, Equation 1 yields an average ratio of tested-to-predicted strength (RTPS) of 0.95 with a coefficient of variation (COV) of 0.11 if the F_{uh} is computed using Eq. 2, and a RTPS of 0.97 and a COV of 0.10 if F_{uh} is taken as 260 ksi.

3.2 PAF PULL-OUT

The basis for establishment of pull-out strengths in the United States represent the code referenced test procedure standard, and an evaluation criteria, typically ASTM E 1190 (ASTM 2008b), and AC70 (ICC-ES 2010), respectively. In European practice, both the testing provisions and evaluation criteria are contained in CUAP (DIBt 2004), which is more specific than its U.S. equivalents in that it is also defines the application scope. The basis for establishment of the PAF pull-out represents the most dominant and most tested mode of failure among all types of PAFs and in nearly all connection configurations. The nature and specific mechanics of pull-out in PAFs is very unique given their specific design features and resistance mechanics. Pull-out strength is derived from the partial fusion stresses, f_f, and hoop confinement stresses, f_c, that result in resistive friction stresses, μf_c. A mechanical model that could be used to determine the pull-out strength of pins is represented graphically in Fig.3. In this particular case, the Fig. 3 considers the embedment case II from Fig. 4.

As can be seen, the pull-out resistance, T_p, can be defined as a mathematical function (Eq. 3) by integrating resisting stresses along the embedded surface of the PAF. Unfortunately, the solution of the integral given in Eq. 3 is a complicated polynomial requiring significant computing effort. Also, Eq. 3 would require modification when embedment condition changes to one of four other possible cases (I, III, IV and V in Fig. 4).

A further complication and found to be impossible to codify is the minute, but varying differences present in the geometric features that seem to have a profound impact on the PAF capacity in pullout. For instance, PAF points and shank knurling are one of the most dominant features impacting pullout resistance sometimes resulting in a pullout strength twice that of a non-knurled fastener of a similar diameter (ITW Ramset 2009). However, virtually every knurled PAF examined in this study featured a unique knurling pattern, each of which was based on a proprietary manufacturer's design. Further, specific metallurgical properties of PAFs and the embedment material, including weldability, hardness, carbon content, etc. cannot be codified in a comprehensive and general form, although each may have a minor to significant impact on the PAFs ability to partially fuse to the embedment hole surface, as well as on the ability of the displaced embedment material to confine the fastener.

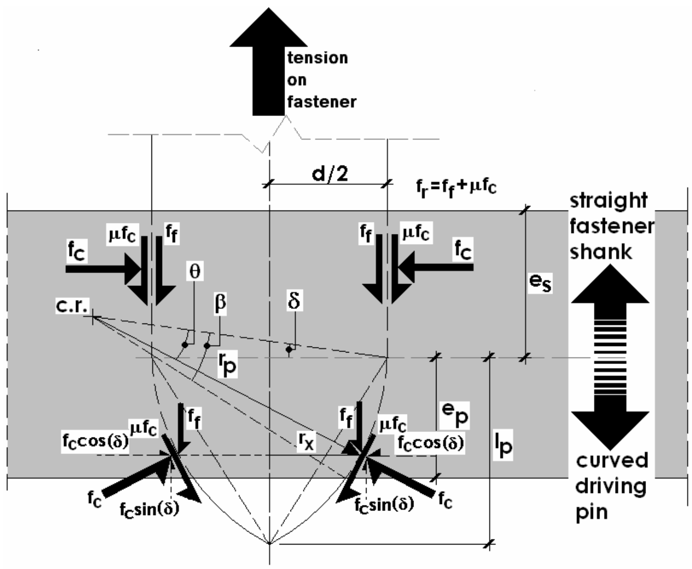

Figure 3 Pullout Strength Mechanical Model for PAFs

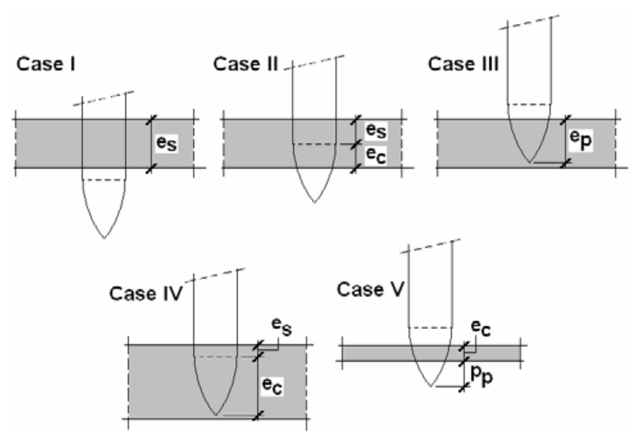

Figure 4 PAF Embedment Cases

$$T_p = f_r \pi e_s \left(\frac{d_s}{2} \right)^2 + \int_0^\beta f\left(d_s, l_p, f_r, e_s, e_p\right) d\theta \qquad \text{(Eq. 3)}$$

In short, while unique values of μf_c and f_f might be successfully determined for one fastener, an entirely different set of values may apply to another pin. As a final point, many PAFs have very complex geometric features affecting pullout strength, such as multiple point diameters, sloping shanks, multiple shank diameters, etc. Capturing all such features in a code-based equation would be an impossible task.

All the above facts render the concept embodied in Fig. 3 and Eq. 3 practically obsolete. Behavior and parametric impact on PAF strength was extensively studied by Beck & Reuter (2005) who found that the PAF pull-out strength depends heavily on depth of penetration. Fig. 5 shows the plot of strength vs. penetration distance for 127 tests of a particular PAF examined in this study. As can be seen, the data appears dispersed in three distinct clouds, with data confined by boundary A distinctly supporting findings by Beck & Reuter (2005). The data outside the boundary A appears also related to penetration distance, but nonetheless also affected by a system effect, including excessive driving energy which was found to have a significant deteriorating effect on pullout strength (Beck & Reuter 2005).

Where PAF points fully penetrate the embedment material (i.e., Case I in Fig. 4), correlation can be found between the embedment length and pull-out strength. This is illustrated in Fig. 6, which depicts such a correlation for 60 tests of a fastener installed in three different thicknesses. The intercept of the trend line in Fig. 6 is zero; therefore there is a direct correlation with the embedment length. However, Beck & Reuter found that although this correlation exists, the strength is not directly proportional to the embedment area of contact.

Based on the limitations presented above, it is clear that a comprehensive generic strength prediction model for PAF pullout is not possible, and that PAF strength in pullout should be determined through testing. As a matter of practical convenience, however, it seemed useful to generate a lower bound solution whereby strength of a smooth shank PAF can be presented in a tabular form for several typical applications. For the purpose of this study, this lower bound is defined as the largest capacity that can be justified for all smooth shank fasteners of the same diameter and the same embedment for which a factor of safety of 3.0 can be justified.

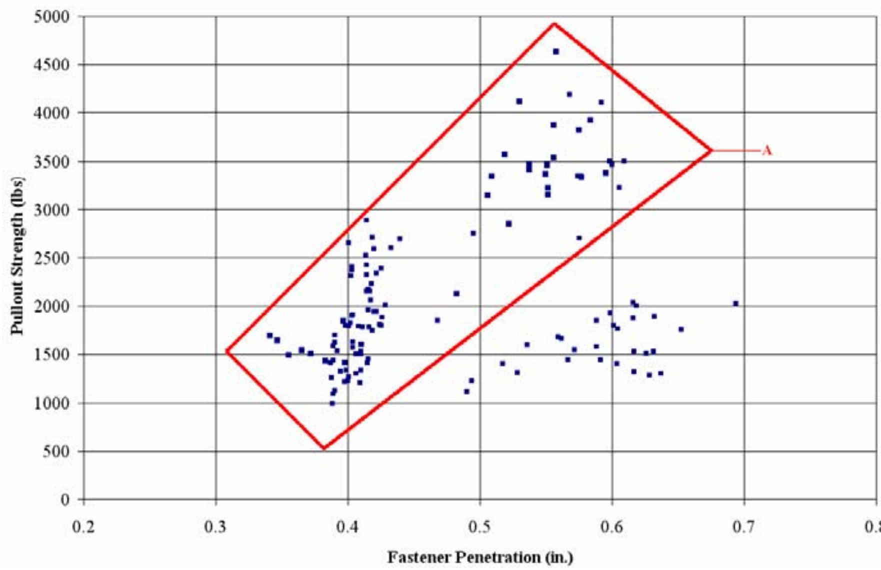

Figure 5 Depth of Penetration vs. Pull-out Strength

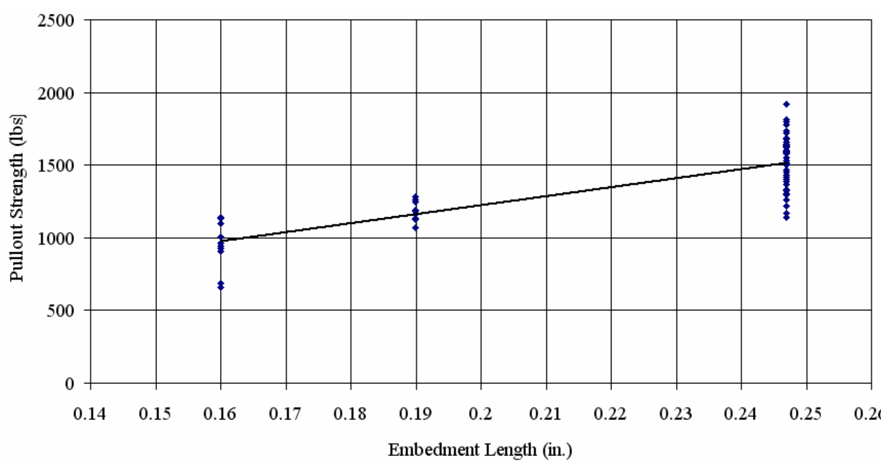

Figure 6 Embedment vs. Pull-out Strength

Table 1 summarizes such strengths based on analysis of 854 tests featuring 13 smooth shank fasteners from all four manufacturers, and then reduced based on applicability limits and typical system effect considerations. Table 1 can safely be applied to knurled shank fastener connections, although only smooth shank fastener tests are in its development. Knurled PAF tests were omitted to avoid erroneous application of the safe table loads to knurled fasteners not covered by this study. Furthermore, Table 2 stipulates shank embedment (i.e., Case I in Fig. 4). Many fasteners do not achieve shank embedment in plates exceeding 5/16 in. in thickness, but rather some portion of, or the entire, PAF point becomes an embedded part of the fastener, often causing failure at lower loads than PAFs with shank embedment in 1/4-in. thick plates. Embedment is the function of a fastener's ability to penetrate a steel member, which in turn depends on the relative hardness difference between the PAF and the embedment material, power-actuated tool settings and driving energy, manufacturer or project specifications, etc. As the objective of this approach is the ability to conveniently and rapidly determine a safe load, rather than supercede actual tested strength reported by the manufacturer, the lower tested strengths corresponding to embedment I, III-V (Fig. 4) have been used to develop the Table 2; however, full embedment (Case I in Fig. 4) is stipulated to avoid unconservative outcomes pertaining to partial embedment and geometries not captured in the data available to this study. It is emphasized that the values provided do not assure the same degree of safety across the board, but rather only assure that the application of factor of safety of 3.0 will ensure the minimum degree of reliability for connections per Chapter F of AISI S100-2007. This solution is intended as a convenient tool for either preliminary or rapid safe design, rather than an alternative to tested pull-out date where available. The manufacturer's applicability limits and installation requirements must be adhered to, and they may preclude the usage various diameter-plate thickness combinations for a particular fastener.

Table 1 PAF Lower Bound Nominal Design Values

	Embedment Plate Thickness, in.		
d_s, in.	1/8	3/16	1/4
0.11-0.15	450	915	1230
0.18-0.21	-	-	1970

3.3 SHEET PULL-OVER

Fundamental behavioral aspects with respect to the pull-over limit state in PAF connections are basically identical to those of pull-over in screw connections. The geometric and other properties affecting the strength are, with exception of fastener head geometry, solely a function of top connected member subject to pull-over. This study found three distinct behavioral types with respect to predicting pull-over strength. Specifically, the pullover strength featuring PAFs with distinct shank and head with or without a washer that does not appreciably differ from screws in their appearance (D, E, and F from Fig. 1) is predicted very well with the model presently contained in Sec. E4.4.2 of AISI S100-2007. A second type represents the connections with PAFs that derive their pullover strength from friction and interlocking of a loose washer with tapered fastener head. This type of fastener is shown as Types A and B in Fig. 1. Essentially, depending on the proportions of the fastener head, the pull-over load will cause the loose washer to ride up the tapered head and lock in place when the washer opening equals head diameter. The fasteners of Type A (Fig. 1) investigated in this study for which $\boldsymbol{a/d_s \geq 1.6}$, and $\boldsymbol{a - d_s \geq 0.12}$ **in.**, consistently achieved the full strength predicted by AISI S100-2007 Sec. E4.4.2, while those with $\boldsymbol{a/d_s \geq 1.4}$, and $\boldsymbol{a - d_s \geq 0.08}$ in. achieved only about 80% of that strength. There is no basis for establishing the strengths for other head proportions for this type of fasteners from the standpoint of the data available to this study, and such strengths should be addressed through testing. Finally, the third type of behavior observed relates to fasteners with compressible spring washers (Type C in Fig. 1). The top of the mushroom shaped washer (although other shapes are available as well) partially collapses when the PAF is installed into the steel member, thus creating an elastic-spring like mechanism that restrains the member subject to pullover in the vicinity of the fastener confined over an area corresponding to the diameter of the washer bottom, as illustrated in Fig. 7. Specifically, the image on the left represents a typical screw-like fastener, whereby a washer deforms along with the top member until distortions in the washer and top member around the hole and/or fastener head are large enough for the tearing and pull-over to occur. The image to the right depicts a fastener with collapsible spring washer.

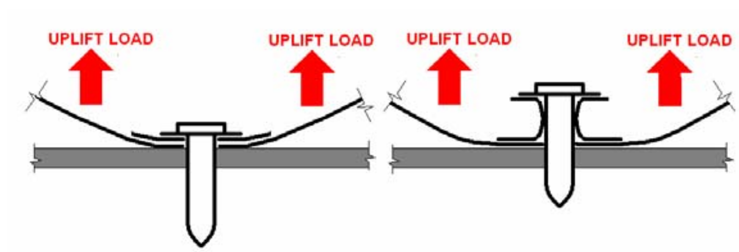

Figure 7 Mechanics of Pull-Over in Power Actuated Fasteners

As can be seen, the washer effectively extends the perimeter of the pull-over failure plane, and thus increases pull-over capacity, by clamping the member in contact with a washer to the base material. This type of fastener consistently yielded connection pullover strengths about 30% higher connection pull-over strengths than that predicted by the AISI S100-2007 model. The model predicting pull-over strength, P_{nov}, can therefore be summarized as shown in Eq. 4.

$$P_{nov} = \alpha_w t_1 d'_w F_{ut1} \qquad \text{(Eq. 4)}$$

where:

α_w = 1.5 for screw-, bolt-, and nail-like flat heads, with or without head washers (Fig. 1, Types D-F)
= 1.5 for threaded stud pins and for pins with tapered standoff heads that achieve pull-over by friction and locking of the loose washer with the pin head (Fig. 1 Types A and B, with a/d_s ratio of no less than 1.6 and $(a - d_s)$ of no less than 0.12 in. (3 mm).
= 1.25 for threaded stud pins and for pins with tapered standoff heads that achieve pull-over by friction and locking of the loose washer with the pin head (Fig. 1 Types A and B, with a/d_s ratio of no less than 1.4 and $(a - d_s)$ of no less than 0.08 in. (2 mm).

t_1 = thickness of member in contact with the fastener head, in.
= 2.0 for pins with collapsible spring washer (Fig. 1, Type C).

d'_w = actual diameter of the washer or the fastener head in contact with the retained substrate. It shall not exceed 0.60 in. (15 mm) in computations, although the actual diameter may be larger.

F_{ut1} = ultimate tensile strength of the member in contact with fastener head (psi)

Figure 8 shows a very good agreement of tested and predicted data. The strength computation model presented as Eq. 4, based on 198 tests on 4 different fasteners, yields an average RTPS of 1.08 and a COV of 17%.

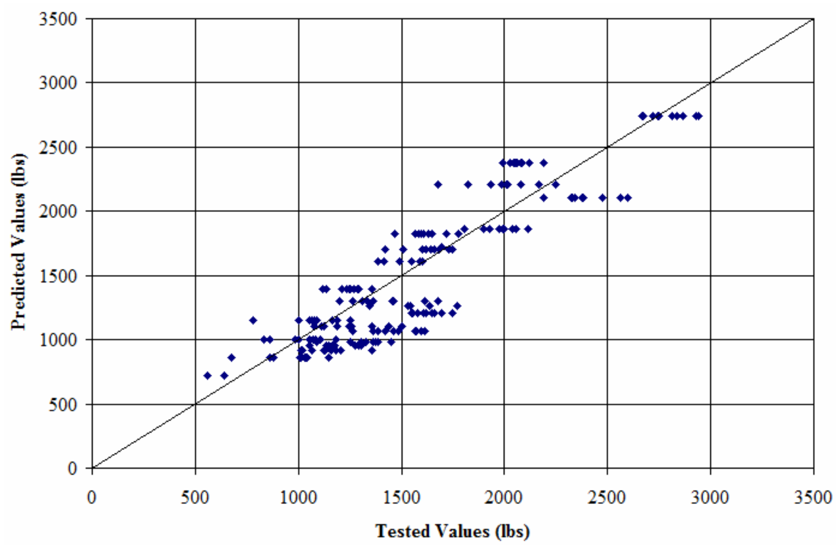

Figure 8 Distribution of Predicted vs. Tested Pullover Strengths

The pullover tests available to this study did not feature any of the blunt-head or sharp-head threaded studs (G through J in Fig. 1). However, in the opinion of the authors, and considering the experimental evidence of other types of fasteners, such fasteners can be considered using Eq. 4 if the variable d'_w is defined as shown in Fig. 2.

4 SHEAR LIMIT STATES

The modes of failure observed in tension PAF test reports are PAF pull-out in shear, shear fracture, bearing, net section strength, and connection strength limited by edge distance. The subsequent sections discuss each of the applicable limit states, and the analysis pertaining thereto.

4.1 SHEAR FRACTURE

The shear fracture strength of a PAF can be computed using Eq. 5. The determination of F_{uh} is discussed in Section 3.1.

$$P_{nsp} = 0.6(d_s/2)^2 \pi F_{uh} \qquad \text{(Eq. 5)}$$

Equation 5, assessed on the basis of 304 tests featuring 14 different fasteners with diameters ranging from 0.106 – 0.197 in., yields a mean RTPS of 1.14 and a COV of 19% if F_{uh} is computed using Eq. 2, and a RTPS of 1.16 and a COV of 19% if F_{uh} is taken as 260 ksi. Distribution of predicted to tested strengths are depicted in Fig. 9. As can be seen, Eq. 5 tends to be more conservative for PAFs with higher nominal strengths. This can be explained by the fact that at higher loads PAF rotation becomes significant, thereby the fastener becomes loaded in a combination of shear and tension. Since the tensile strength of a fastener is larger, these fasteners yield a higher overall capacity. This, however, is also dependent on the size of the embedment member, which facilitates rotation when it is relatively flexible. From a practical standpoint, and attempting to maintain model simplicity, this phenomenon need not be considered, as typical connections with very high shear fracture strength will typically yield a lower strength due to another governing limit state.

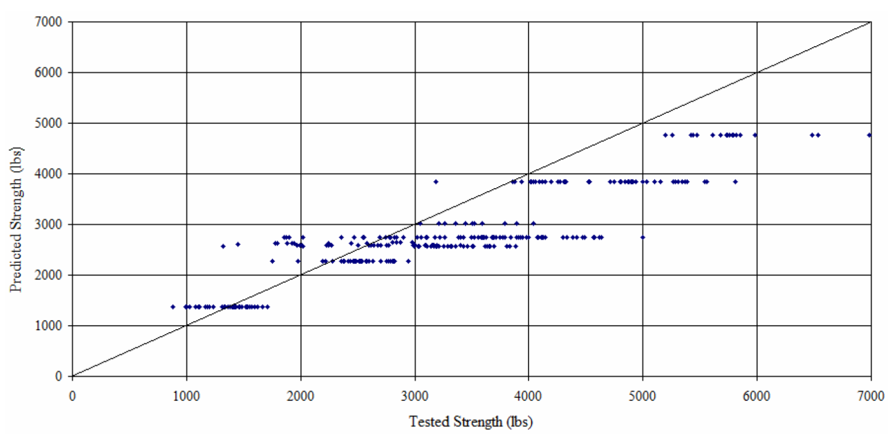

Figure 9 Distribution of Predicted vs. Tested Pullover Strengths

4.2 SHEAR PULL-OUT

Shear pull-out is a limit state widely reported in shear tests. It is an ultimate consequence of fastener tilting associated with significant deformations in the embedment base steel member. Given the configuration of the test setup, nearly all shear pullout test data available to this study reported only the thickness of one member thickness (i.e., PAF is installed into only one member). Therefore it was not possible to assess the ratio t_2/t_1 at which bearing transitions into tilting for any given fastener. Also, several test groups contained both test samples failing in bearing and shear pull-out, thus indicating that pullout in shear is possible even at higher t_2/t_1 ratios. The approach taken in this study was to develop an equation for bearing that would be applicable to connections with t_2/t_1 of 2 or greater, which was the range of available data with reported bearing failure (Section 4.3).

Another equation predicting the PAF pull-out in shear was developed over the entire range of available data over which such a failure was reported. Specifically, 237 tests, featuring 7 fasteners ranging from 0.106 – 0.206 in. in diameter embedded in members of thicknesses ranging from 0.113 – 0.75 in., for which pull-out in shear was a reported mode of failure, and for which the strength properties of the embedment material and the fastener embedment condition was reported, were isolated and used in the equation development. The AISI S100-2007 equation for prediction of tilting strength in screws was found inapplicable, as it provided a very poor fit with the available data over nearly the entire range. However, the model developed by Mujagic et al. (2007) for predicting the shear pull-out strength in standoff screws was found to provide an excellent match with the data. This model is presented as Eq. 7. Some of its constants were slightly modified to provide the best statistical fit with the data. Fig. 10 shows the distribution of tested to predicted strengths for shear pull-out. The model presented as Eq. 7 yields an average RTPS of 1.03 and a COV of 17%.

$$P_{nos} = \frac{d_{ae}^{1.8} t_2^{\,0.2} \left(F_{y2} E^2\right)^{1/3}}{95} \qquad \text{(Eq. 7)}$$

where:

F_{y2} = yield strength stress of the member not in contact with fastener head, psi

E = elastic modulus of steel = 29000 psi

d_{ae} = average embedded PAF diameter, in.
= d_s when e_s in Fig. 4 equals t_2

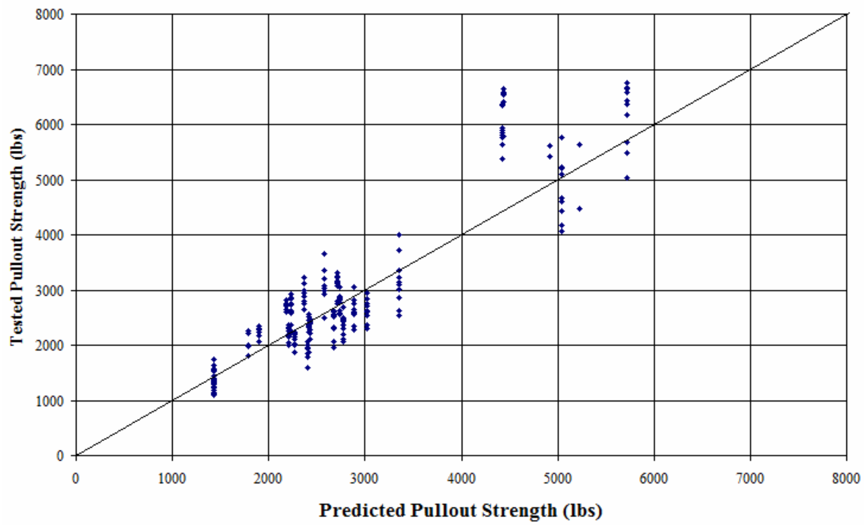

Figure 10 Distribution of Predicted vs. Tested Pull-out Strengths

4.3 BEARING, EDGE DISTANCE, SPACING AND NET SECTION CHECKS

The spacing and edge distances reported for many of the test specimens considered were in the order of 8 to 10 times the PAF shank diameter. Such large distances are considered excessive, and in many practical situations difficult to achieve. The ASTM standard governing testing procedures for power-actuated fasteners, E 1190-1995/2007 (ASTM 2008) provides a set of edge and spacing distances deemed to eliminate the effects of fastener grouping and edge distance. These limits are summarized in Table 2, and are recommended with the application of this strength prediction model.

Table 2 Minimum Required Edge and Spacing Distances

Pin Shank Diameter (in.)	Minimum Pin Spacing (in.)	Minimum Edge Distance (in.)
0.100-0.199	1.0	0.5
0.200-0.250	1.6	1.0

It should be noted that the model presented in this paper does not account for the effects of fastener grouping and edge distance on the computed strength, as such effects could not be evaluated from the available data. Therefore, the model cannot be applied to connections not satisfying the limitations of Table 3, whose strength should be established through testing.

Tests reported by Beck and Englehardt (2002) show that the net section strength of a steel member with installed PAFs consistently exceeds the strength of net sections with drilled holes of equivalent diameter. Therefore, the net section checks currently prescribed by AISI S100-2007 for other types of connections can safely be applied to the connections featuring power actuated fasteners. As a result of the same study, the authors recommended that the hole diameter be taken as 1.10 times the pin diameter in net section check calculations. This recommendation has been adopted for use with this model.

Bearing strength is generally defined as the product of fastener diameter, thickness of the bearing material, bearing material ultimate tensile strength, F_{ut1}, and a constant. This constant has values of 2.7 for screws (AISI 2007), 3.2 for power actuated fasteners in EN 1993-1-3 model (ECS 2006), and between 2 and 3 for structural bolts (AISC 2005) depending on edge and hole deformation considerations. Furthermore, in the AISI model, the tilting must be considered when the ratio of thickness of member not in contact with the fastener head, t_2, to the thickness of the member in contact with fastener head, t_1, does not exceed 1. The tilting check does not apply when this ratio equals 2.5 or more, and linear interpolation between the governing strengths at t_2/t_1 of 1 and 2.5 is used to determine the strengths in the intermediate range. Tilting reflects the fact that when two connected members are of similar thickness, connections tend to rotate with respect to the axis of applied force thus tilting the connection fastener which eventually pulls out.

The bearing strength of PAF connections was assessed in this study on the basis of 127 tests featuring 3 fastener models of Type A and C from Fig. 1 . Based on the analysis of the available data, it was shown that a constant multiplier of as high as 4.2 could be justified, which is much higher than in the case of either screws or bolts. The source of this higher strength most likely rests in washer clamping, sheet hardening and folding effects around the perimeter of the hole. However, 3.7 was chosen as the constant multiplier, as shown in Eq. 7.

$$P_b = 3.7 d_s t_1 F_{ut1} \quad \text{(Eq. 7)}$$

Specifically, Fig. 11 depicts the plot or RTPS based on Eq. 8 versus t_2/t_1 ratio. As can be seen, and as expected, as this ratio decreases so does the strength defined solely by the bearing check of Eq. 7, thus indicating presence of tilting at lower ratios of t_2/t_1. Given the relatively limited data space, the actual transition point where tilting applies cannot be determined with certainty. However, if the model is limited to a minimum t_2/t_1 ratio of 2 (minimum for the data available in this study), which covers vast majority of shot fired pin applications, combined with setting the intercept of the average RTPS to about 1.0 for the group of tests with the lowest considered t_2/t_1 ratio (in this case 2), the model can safely predict the bearing and tilting strength without the need for a separate tilting formula. A constant of 3.7 accomplishes this goal. It should be noted that the model represented by Eq. 8 does not require any checks on the member not in contact with the fastener head; since the model is limited to configurations where $t_2/t_1 \geq 2$, bearing on the member not in contact with the PAF head will not govern the connection capacity when this model is used.

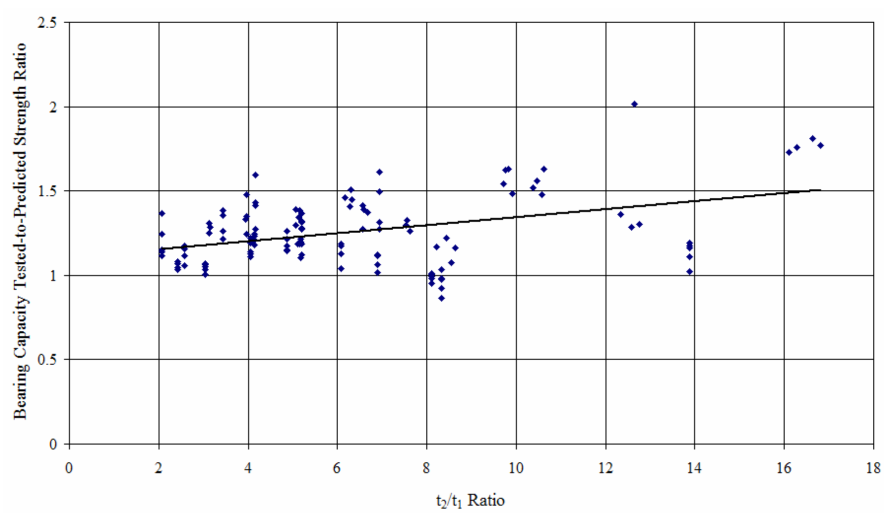

Figure 11 Influence of t_2/t_1 Ratio on Bearing RTPS

In terms of statistical performance over the entire sample group, a mean RTPS of 1.26 and a COV of 0.16 are calculated. For the group of data with t_2/t_1 = 2, the mean RTPS is 1.20 and COV is 0.08. To eliminate bias of any deterministic considerations pertaining to the test sample, the resistance and safety factors for bearing and tilting presented in Section 5 are based on both the overall statistics and those pertaining to the group with t_2/t_1=2.

The test database featured fastener diameters ranging from 0.146 – 0.177 in. and top member thickness ranging from 0.018 to 0.06 in. Furthermore, based on the range of the test sample, Eq. 8 should be used only when $t_2 \geq 1/8$ in.

5 RELIABILITY ASSESSMENT AND SAFETY PROVISIONS

The resistance and safety factors for the limit states investigated in this study were established using the first-order second-moment reliability method presented in Chapter F of AISI S100-2007. The professional factor, P_m, was varied based on the actual RTPS. The materials factor, M_m, was taken as 1.10, and its coefficient of variation, V_M, was taken as 0.10 for all limit states except for bearing and pull-out in shear, where V_M = 0.08. The fabrication factor, F_m, and its associated coefficient of variation V_F, were taken as 1.00 and 0.05, respectively, for all limit states except for bearing and tilting, and pull-out shear, where V_F was taken as 0.05. The reliability index, β, of 3.5 was considered for U.S. applications and β of 4.0 was considered for Limit States Design (LSD).

The above values match those provided for screws in AISI S100-2007 Chapter F. They can be justified by relative comparisons of statistical indices of screws and PAFs. Specifically with respect to M_m and V_M, materials used in manufacturing screws are very similar. While PAFs are typically made of hardened AISI 1060 - 1080 steels, screws are typically made using similar AISI 1018 – 1040 steels using identical case hardening technology. Lower V_M for bearing and tilting is justified, as the value of 0.08 corresponds to the strength properties of mild steels typically found in supporting members associated with PAFs (Galambos & Ravindra 1978), and bearing and tilting and shear pull-out checks are depended on the strength properties of the supporting material, rather than those of the fasteners.

With respect to fabrication parameters F_m and V_F, PAFs again appear at no disadvantage to screws. A review of typical shop drawings for screws (Sealtite 2006) with those of PAFs (HILTI 2009, ITW Buildex 2009) indicate similar, or in some more conservative, fabrication tolerances for PAFs when compared to the screws. Furthermore, minute geometric features of PAFs, such as knurling and point geometry, are critical to their performance, particularly in tension pullout, and are manufactured to tighter tolerances than any specific features associated with screws. Manufacturers generally monitor the COV of individual test groups throughout testing protocols. Those with COV in access of 15% are closely studied, and design features are often adjusted to achieve greater consistency and reliability.

Fig. 12 depicts a distribution of COV for 114 pullout groups of tests, with each group comprising between 5 and 30 tests. With a P_m of 1.0 and a COV of approximately 0.21 will result in a factor of safety of 3.0. As can be seen, 81% of this, essentially random, sample available to this study would fall into this group, while 97% of the test groups would fall within a COV of 0.30, which approximately corresponds to a factor of safety of 4.0. Therefore, while actual manufacturer's data should be used to establish a factor of safety where the design capacity is derived from tests, a factor of safety of 4.0 could safely be applied to the manufacturer's data where the average tested strength is provided, but statistical indices were not. As can be seen from the COVs reported throughout this paper from individual limit states, the proposed strength prediction models yield COV in most cases well under 0.20. Table 3 summarizes the resistance and safety factors for all limit states considered in the paper.

From the standpoint of reliability and statistical performance, the authors believe that statistical indices presented herein show that PAFs represent a viable alternative to screws for the attachments of mechanical and architectural components to steel members even in regions with higher Seismic Design Categories. The viability of this alternative would be consistent with the current and past use of PAFs for attachment of cold-formed steel deck diaphragms and shear walls for resisting seismic forces. Furthermore, recent research on seismic behavior of fastenings in diaphragms (Essa et al. 2002) found energy-dissipation properties of PAF connections vastly superior to those of welded or screw connections.

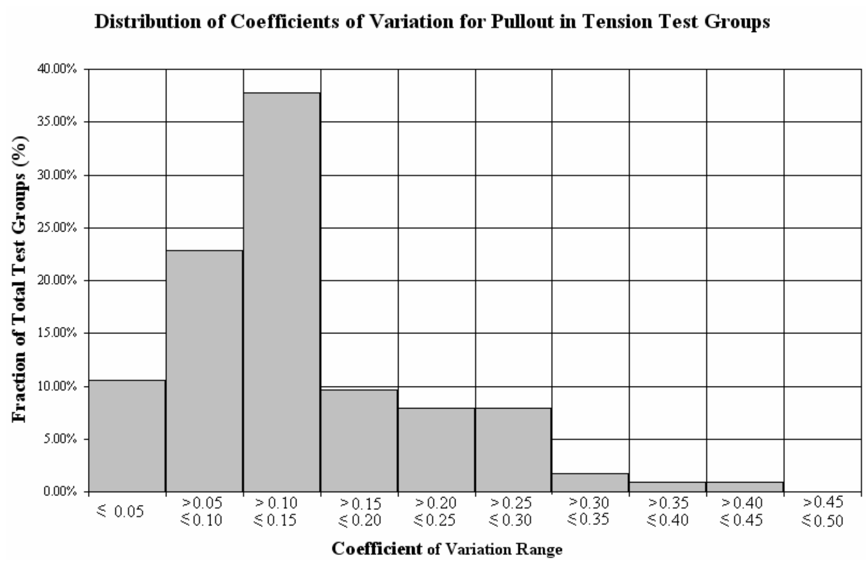

Figure 12 Distribution of COV from 114 Test Groups

Table 3 Resistance & Safety Factors for Power Actuated Fasteners

LIMIT STATE	ϕ	Ω	ϕ_{LSD}
Tension Fracture*	0.60	2.65	0.50
Tension Pullout Table 1 Strengths Tested Strengths	 0.55 Calculated per AISI S100-2007 Ch. F or 0.40	 3.00 Calculated per AISI S100-2007 Ch. F or 4.00	 0.45 Calculated per AISI S100-2007 Ch. F or 0.30
Tension Pull-Over	0.60	2.70	0.50
Shear Fracture	0.60	2.65	0.50
Shear Pull-Out	0.65	2.55	0.50
Bearing & Tilting	0.80	2.05	0.65

*Established based on shear fracture tests due to insufficient tensile fracture test sample size. This is conservative, as shear fractures are typically associated with more statistical scatter than tension fractures.

6 SUMMARY AND CONCLUSIONS

The goal of this study was to generate a strength prediction model for power actuated fasteners embedded in steel members, and loaded in shear and tension. The study presents such a model based on an analysis of test reports of four major manufacturers of power actuated fasteners in North America (HILTI, ITW Buildex, Powers Fasteners, and Simpson). The generated strength prediction model is presented in format conducive to its adoption in a North American Code such as AISI S100. The analysis indicates that power actuated fasteners represent a viable alternative to screws within the scope of applications covered by this analysis. This study does not address the effect of fastener groupings or combined shear-tension loadings.

The authors suggest a future comprehensive research effort that would address combined loading checks, investigate the effect of fastener grouping, extend the applicability of the model proposed herein to a wider range of variables and assess the PAF attachments of steel members to other materials.

7 ACKNOWLEDGMENTS

The authors extend their sincerest gratitude to HILTI, ITW Buildex, Powers Fasteners and Simpson for graciously supplying the test reports on which this study was based. The authors also wish to thank AISI and its Technical Manager Dr. Helen Chen for their tireless efforts in coordinating and assisting with this study.

8 REFERENCES

AISC (2005) "Specification for Structural Steel Buildings," American Institute of Steel Construction, Chicago, IL.

AISI (2007) "S100-2007 North American Specification for the Design of Cold-Formed Steel Structural Members" American Iron and Steel Institute, Washington, DC.

ASTM (2008a) "Standard Specification for Steel Bars, Carbon and Alloy, Hot-Wrought, general Requirements for," ASTM Standards in Building Codes, Volume 4, 45th Edition, pp. 64-79.

ASTM (2008b) "E 1190-95 (Reapproved 2007) - Standard Test Methods for Strength of Power-Actuated Fasteners Installed in Structural Members," ASTM Standards in Building Codes, Volume 4, 45th Edition, pp. 615-620.

ASTM (2009) "A 370-09 Standard Test Methods and Definitions for Mechanical Testing of Steel Products," ASTM Standards in Building Codes, Volume 1, 45th Edition.

Beck, H. and Engelhardt, M.D. (2002) "Net Section Efficiency of Steel Coupons with Power Actuated Fasteners," ASCE Journal of Structural Engineering, Vol. 128, Number 1, pp. 12-21.

Beck, H., Engelhardt, M. and Glaser, N. (2003) "Static Pullout Strength of Power Actuated Fasteners in Steel: State-of-the-Art Review," AISC Engineering Journal, 2nd Quarter, pp. 99-110.

Beck, H. and Reuter, M. (2005) "Powder-actuated fasteners in steel construction," 2005 Steel Construction Calendar, Berlin, Germany.

BSI (1967) "BS 860:1967 Tables for comparisons of hardness scales," BSI, London, UK.

DIBt (2004) "Common Understanding of Assessment procedure (CUAP) - Cartridge fired pin for connections for thin gauge steel members and sheeting" Deutsches Institute für Bautechnik, Berlin, Germany.

ECS (2006) "Eurocode 3 – Design of steel structures - Part 1-3: General Rules – Supplementary rules for cold-formed members and sheeting (EN 1993-1-3)," ECS, Brussels, Belgium.

Essa, H.S., Tremblay, R., and Rogers, C. (2002) "Inelastic Seismic Response of metal Roof Deck Diaphragms for Steel Building Structures, Proceedings of 12th European Conference on Earthquake Engineering, European Association for Earthquake Engineering, Elsevier, Oxford, UK.

Galambos T.V. & Ravindra, M.K. (1978) "Properties of Steels for use in LRFD," Journal of Structural Division, ASCE, Vol. 104, No. ST9, pp. 1459 – 1468.

HILTI (2008) "North American Product Technical Guide – A guide to specification and installation," Tulsa, OK.

HILTI (2009) Electronically submitted test data for power-actuated fasteners to AISI (Not For Distribution), HILTI, Tulsa, OK.

HILTI (2010) Electronically submitted test data for power-actuated fasteners to AISI (Not For Distribution), HILTI, Tulsa, OK.

ICC-ES (2010) "Acceptance Criteria for Fasteners Power-Driven into Concrete, Steel, and Masonry Elements (AC70)" International Code Council Evaluation Service, Inc., Whittier, CA.

ITW Ramset (2009) Electronically submitted test data for power-actuated fasteners to AISI (Not For Distribution), ITW Ramset, Glendale Heights, IL.

ITW Ramset (2007) "Ramset Performance/Submittal Information" ITW Ramset, Glendale Heights, IL.

Mujagic, J.R.U., Easterling, W.S., Murray, T.M. (2007) "Drilled Standoff Screws for Shear Connection in Light Composite Trusses," Journal of Constructional Steel Research, Vol. 63, Issue 10, pp. 1404-1414.

Powers Fasteners (2009) Electronically submitted test data for power-actuated fasteners to AISI (Not For Distribution), Powers Fasteners, Brewsters, NY.

Sealtite (2006) "Sealtite Building Fasteners – Technical Data: Performance Data Charts, Laboratory Test Reports & Laboratory Test Methods," Sealtite Building Fasteners, Tyler TX.

Simpson Fasteners (2009) Electronically submitted test data for power-actuated fasteners to AISI (Not For Distribution), Simpsons Fasteners, Pleasanton, CA.